

Effect of superimposed oscillations on the creep characteristics of Al-22 wt%Ag alloy

M. A. MAHMOUD, G. GRAISS

Physics Department, Faculty of Education, Ain-Shams University, Cairo, Egypt
E-mail: moustafa_a_mahmoud@hotmail.com

The behavior of both transient and steady state creep of Al-22 wt% Ag alloy was investigated using a constant stress in the aging temperatures range 423 to 683 K where torsional oscillations of different frequencies and amplitudes were operated at various testing temperatures. The subsequent decrease and increase in the creep parameters, n , β and ε_{st} with increasing aging temperatures has been explained on the basis of structure transformations occurring in Al-Ag system and their mode of interaction with mobile dislocations created by the applied stress and the imposed oscillations. An augment in both transient and steady state rates was observed by increasing both frequency and amplitude of the applied oscillations. Dislocation intersection mechanism is assumed as the rate controlling mechanism for both creep stages. © 2002 Kluwer Academic Publishers

1. Introduction

Al-Ag alloys are heat-treatable alloys, which may be strengthened or softened by giving them a special type of heat treatment to produce a special series of useful engineering materials. The sequence and mechanism of structure transformation in a supersaturated solid solution of Al-Ag system is known [1] to be: spherical G.P zones (tetrahedral) \rightarrow metastable γ' -phase \rightarrow equilibrium γ -phase (hcp). The early stages of decomposition of solutionized Al-Ag system start by formation of the ordered η -state of G.P zones below 443 K [2]. Above this temperature a disordered ε -state is developed [3]. In a sample of Al-4.5 at.% Ag alloy aged at temperatures up to 498 K, where coarser G.P zones exist, reversion into a plate-like metastable γ' -precipitates takes place [4]. For later stages, the equilibrium γ -phase (Ag₂Al) evolves [5].

Creep tests with superimposed low frequency oscillations under constant stress fill a significant position in mechanical testing of material. In the course of a previous study by the authors [6] on the effect of the amplitude of cyclic stress reduction on the creep behavior of Al-Ag and Al-Ag-Zr alloys, an acceleration of steady state rate has been noticed. Beshai *et al.* [7], in their work on the creep behavior of Al-Si system noticed that the steady state creep rate showed some sensitivity to the frequencies of vibration applied during creep measurements. However, a systematic study of the effect of torsional oscillations that may be imposed on wires of Al-Ag alloys while subjected to creep has not been studied. Therefore, the present study is undertaken aiming to throw more light on the effect of superimposed oscillations of different low frequencies or different shear strain amplitudes on the creep characteristics of Al-22 wt% Ag alloy.

2. Experimental procedure

Al-22 wt% Ag alloy was prepared by melting pure Aluminum and silver (99.99%) under vacuum in a high-purity graphite crucible. The ingots were homogenized at 823 K for 4 days, then cold-swaged with intermediate anneal into wires of 0.35 mm in diameter and 50 mm long. Prior to testing, all samples were annealed for 3 h at 798 K to eliminate the hardening effect that might be arise during the machining of the samples, then quenched in iced water. Immediately after quenching, the samples were aged for 1 h at different aging temperatures ($T_a = 423, 453, 493, 563, 613$ and 683 K) to cover the transformation regions.

The creep tests have been performed on a suitably designed creep testing machine operating under constant load corresponding to a stress of 56 Mpa and at testing temperatures, T_t of 353, 373, 393 and 413 K with the testing wire in a vertical position. The aging and testing temperatures were monitored with chromel-alumel thermocouples held in contact with the test sample and were maintained to within ± 1 K. The load was applied to the lower end of the sample. The upper end was fixed in a clamp provided with a transverse vane subjected to low frequency oscillatory motion obtained by a motor provided with a group of gears having different diameters—where different low frequency oscillations could be obtained— as described elsewhere [8]. Four low frequencies, ν , of 1.16, 1.5, 2, and 2.5 Hz were used.

Also, the tested samples were affected by shear strain amplitudes, θ , which were calculated using the formula [7]:

$$\theta = \frac{ra}{hL} \quad (1)$$

where r being the radius of the sample, L its length, h is the half-length of the vane, and a is the actual amplitude of the oscillating vane that was measured by a traveling microscope. Preliminary tests were carried out to select shear strain amplitudes, θ , within the elastic limit range [8]. The values of shear strain amplitude, θ selected were $(6.7, 7.8, 9.4 \text{ and } 11.6) \times 10^{-4}$. The creep tests were performed while the oscillations imposed either of different frequencies, ν , with constant shear strain amplitude, θ , or of different shear strain amplitudes under constant frequency, ν .

3. Experimental results

A series of creep curves of Al-22 wt% Ag alloy were obtained for samples aged at different temperatures ($T_a = 423\text{--}683$ K) to produce the desirable microstructures of G.P zones, metastable γ' -phase and the equilibrium γ -phase. Typical examples curves of strain-time relations for samples pre-aged at 423 and 683 K and worked at testing temperature of 413 K are shown in Fig. 1a for samples subjected to superimposed oscillations of different frequencies, ν , with a fixed shear strain amplitude ($\theta = 6.7 \times 10^{-4}$) and Fig. 1b for samples crept under oscillations of different shear strain amplitudes at constant frequency ($\nu = 1.16$ Hz). The relation for samples not subjected to oscillations (static creep) is also induced for comparison. It is clear from Fig. 1 that all the creep curves exhibit normal creep behavior, and the strain level increase as the magnitude of either frequency, ν , or shear strain amplitude, θ , of oscillations increases.

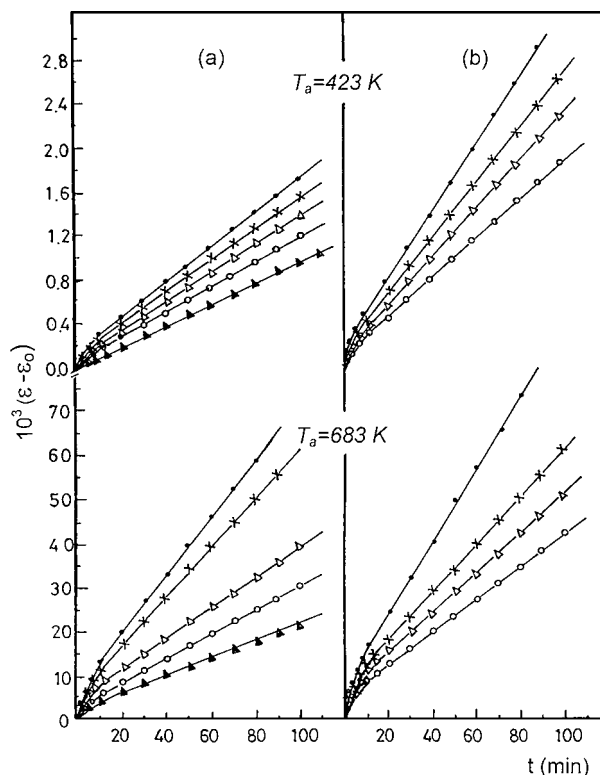


Figure 1(a and b) Representative strain-time curves for Al-22 wt% Ag alloy samples crept under different frequencies, ν , and shear strain amplitudes, θ respectively at testing temperature of 413 K. The applied frequencies are: \blacktriangle 0, \circ 1.16, \triangle 1.5, \times 2 and \bullet 2.5 Hz. The applied amplitudes are: \circ 6.7×10^{-4} , \triangle 7.8×10^{-4} , \times 9.4×10^{-4} and \bullet 11.6×10^{-4} .

As has frequently been reported before [9, 10] the transient creep strain ε_{tr} can be described by the equation:

$$\varepsilon_{tr} = \beta(t_{tr})^n \quad (2)$$

where t_{tr} is the transient creep time (in s). The transient creep exponent n was calculated from the slopes of the straight lines relating between $\ln \varepsilon_{tr}$ and $\ln t$ at different aging and testing temperatures for different magnitudes of ν and θ . The transient creep parameter β was calculated by substitution in the equation:

$$\ln \beta = \ln t_2 \ln \varepsilon_{tr_1} - \ln t_1 \ln \varepsilon_{tr_2} / \ln t_2 - \ln t_1 \quad (3)$$

which is derived from Equation 2. The effect of aging temperature T_a on n and β values is given in Figs 2 and 3 respectively for samples crept under different magnitudes of ν and θ . The steady state creep rate, ε_{st} values evaluated from the slopes of the linear parts of the creep curves of Fig. 1 are given in Fig. 4a for samples crept under different frequencies and Fig. 4b for samples crept under different shear strain amplitudes.

Figs 2–4 imply that:

- The variations in n , β and ε_{st} with aging temperatures, T_a , are quite similar irrespective of the parameters of oscillation applied (ν or θ).
- The sequence of curves with respect to testing temperatures is regular.
- A monotonic shift towards higher values of n , β and ε_{st} is observed with increasing aging temperatures except for samples aged at 453 and 563 K which show a sudden drop followed by a normal increase with further increase of aging temperatures at 613 and 683 K respectively.
- The minima of n , β and ε_{st} values attained at $T_a = 453$ K are generally more deep (i.e. of less values) than those at $T_a = 563$ K, and the following rise in these values is more high at $T_a = 613$ K than at $T_a = 493$ K while a marked increase is obtained at temperature range (613–683 K) and the curves become smoother.
- Under the same conditions of heat treatment, the levels of n , β and ε_{st} in case of applying θ take place with higher values than in case of applying ν .

The dependence of β , n and ε_{st} values on the applied frequency, ν , at $T_t = 413$ K for different values of T_a is shown Fig. 5a–c respectively while Fig. 5d–f concerning the same parameters depending on the different magnitudes of shear strain amplitude, θ . From Fig. 5 it is evident that n , β and ε_{st} values increase with the increase in the magnitude of both ν and θ . In the previous Figures, some n , β and ε_{st} values at $T_a = 613$ and 683 K are not included to allow clearance between curves. T.E.M micrographes investigated by the author for the same alloy and show the existence of fine G.P zones, coarse G.P zones, reversion of G.P zones into metastable γ' -phase, coarse metastable γ' -phase and the equilibrium γ -phase were already published elsewhere [11, 12].

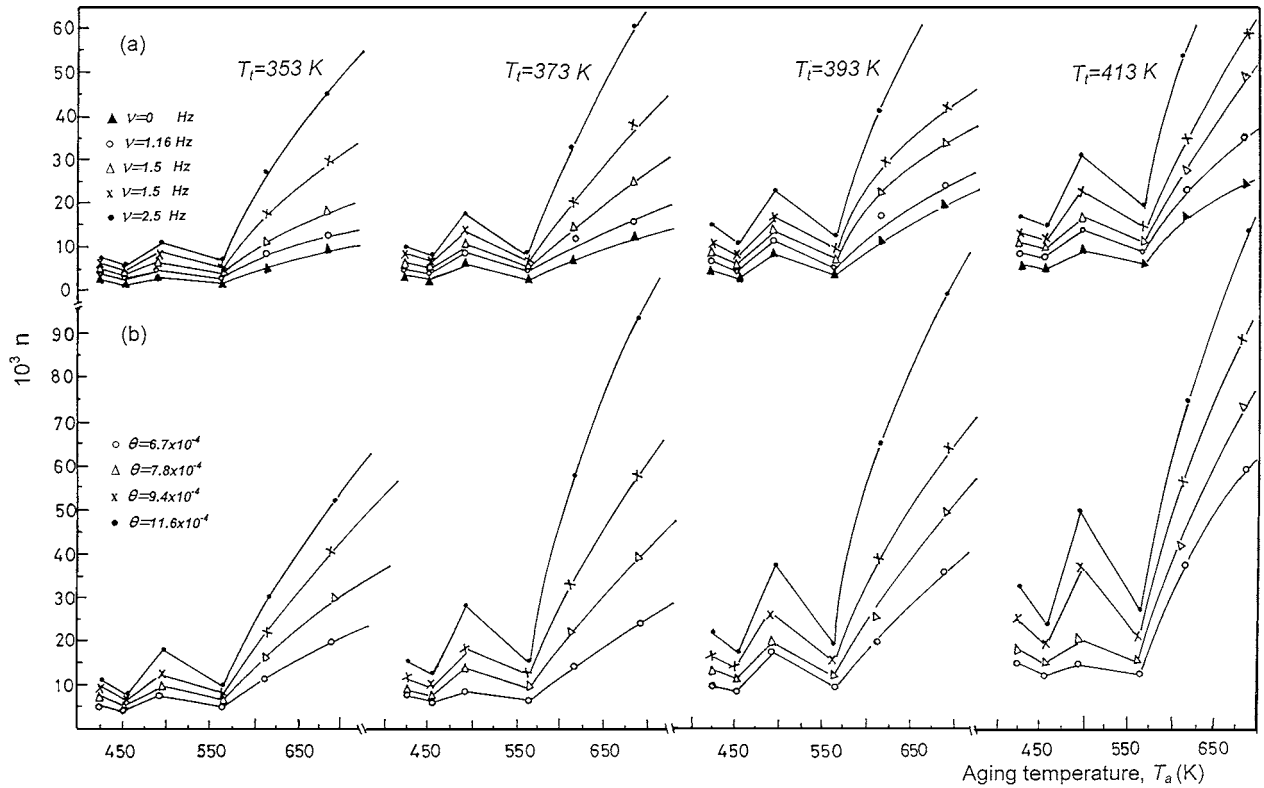


Figure 2 Dependence of transient creep exponent n on aging temperature T_a at: a) different frequencies, ν and b) different shear strain amplitudes, θ . Testing temperatures applied, T_i are indicated.

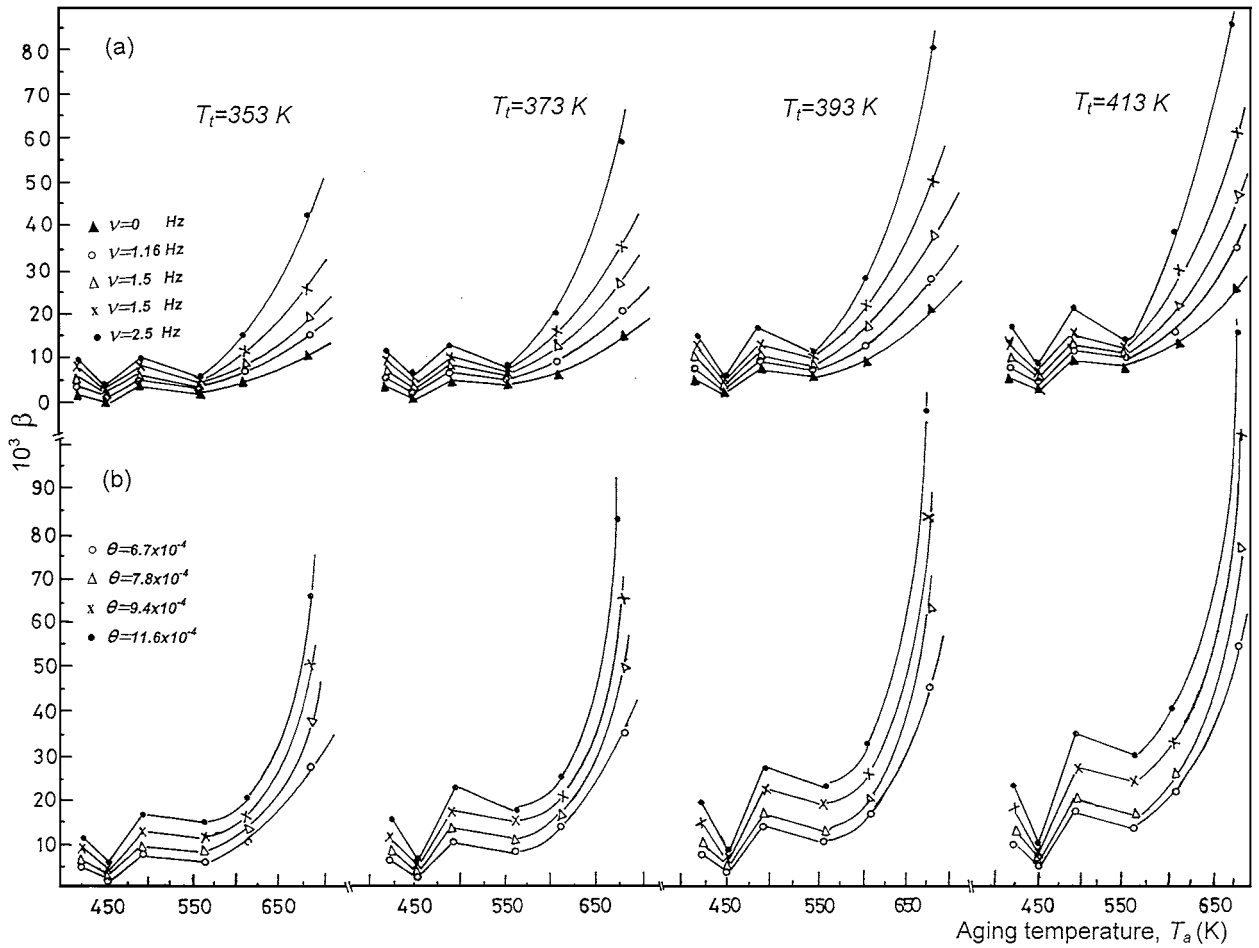
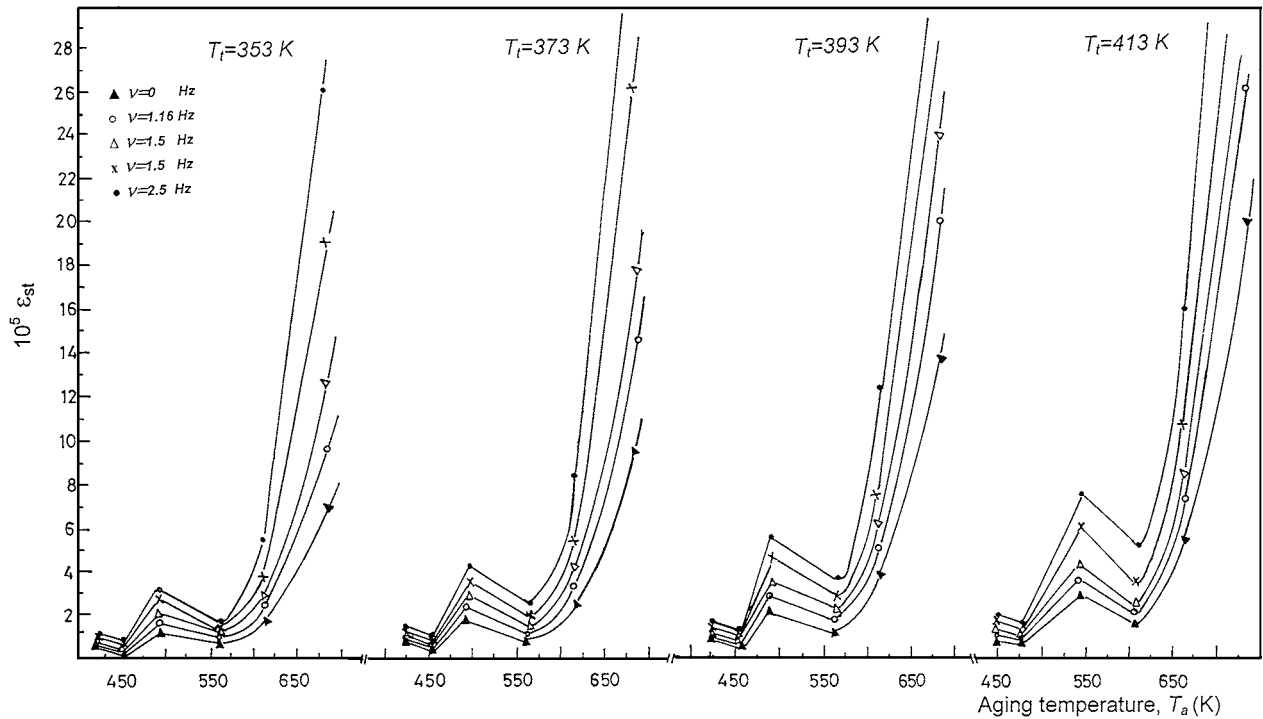
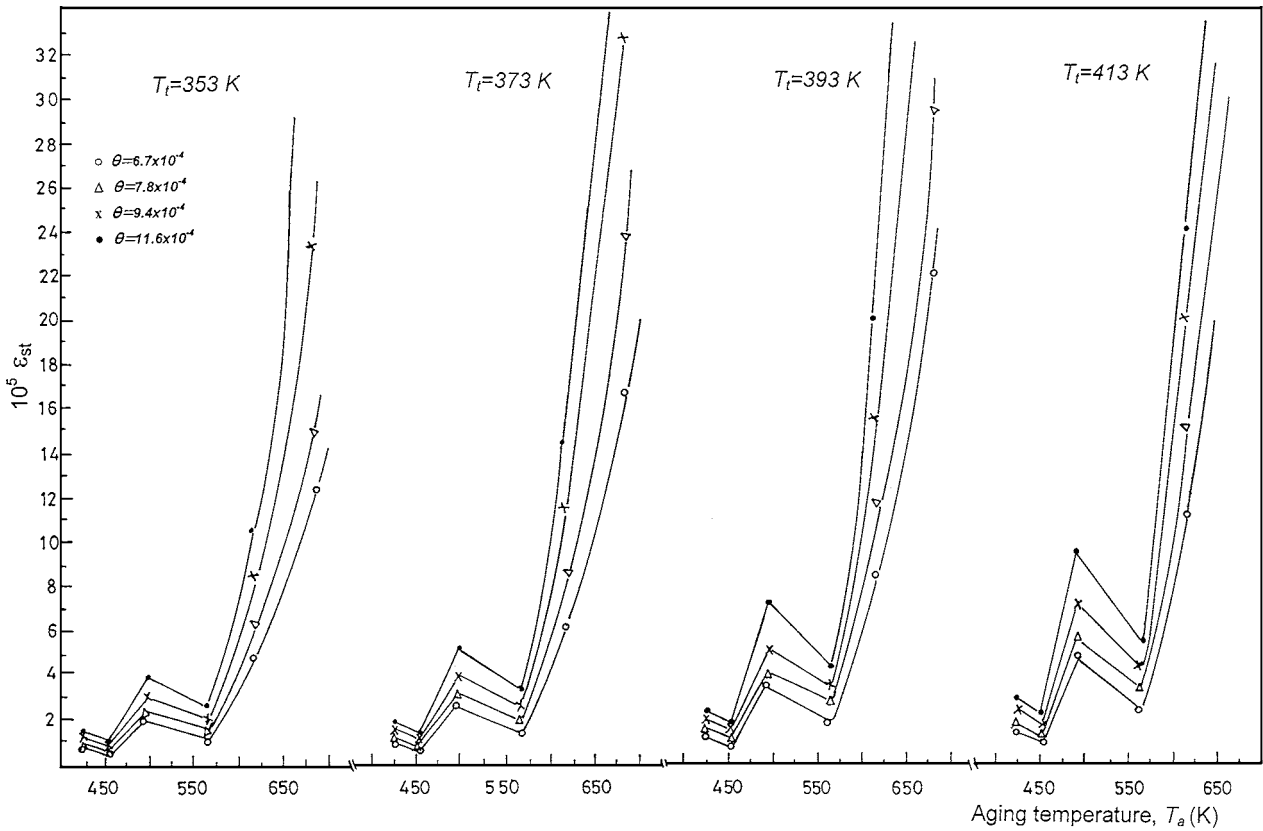


Figure 3 Dependence of the transient creep parameter β on aging temperature T_a at: a) different frequencies, ν and b) different shear strain amplitudes, θ . Testing temperatures applied, T_i are indicated.



(a)



(b)

Figure 4 Dependence of the creep strain rate, ϵ_{st} on aging temperature T_a at: (a) different frequencies, ν and (b) different shear strain amplitudes, θ . Testing temperatures applied, T_t are indicated.

4. Discussion

The characterizing tensile properties of Al-Ag alloy aged at different temperatures depend mainly on the type of the dispersed phase and its interaction with the existing dislocation structure, and the nature of the surrounding matrix [13, 14]. The subsequent decrease and increase in the values of n , β and ϵ_{st} with increas-

ing aging temperatures, as shown in Figs 2–4, can be interpreted on the bases of structural changes occurring in Al-Ag system; G.P zones \rightarrow metastable γ' -phase \rightarrow equilibrium γ -phase, and their interaction with moving dislocations. The slight decrease in n , β and ϵ_{st} values for different values of ν or θ and at all testing temperatures in the lower aging temperatures range 423

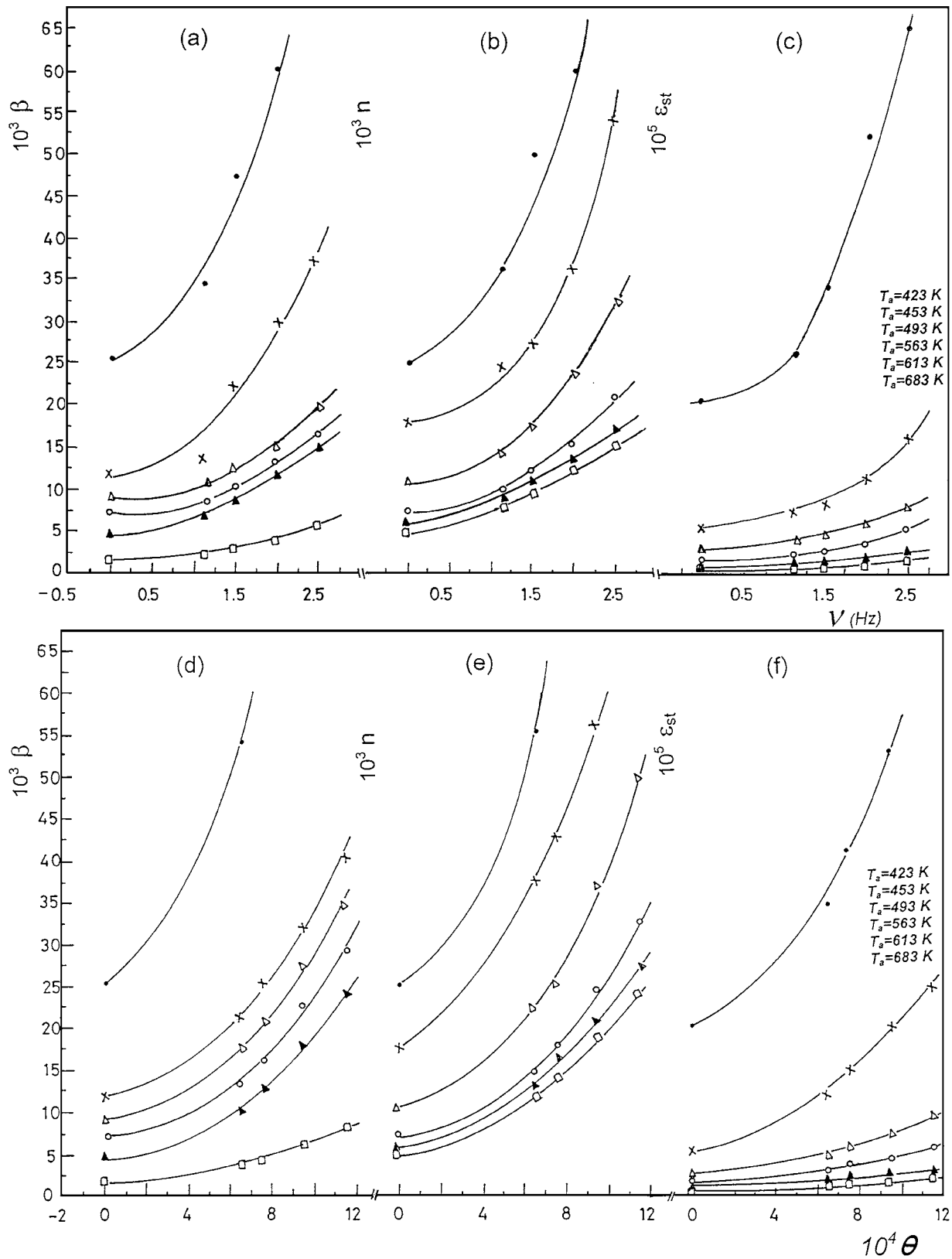


Figure 5(a, b and c) Dependence of transient creep parameter β , transient creep exponent n , and the creep strain rate, ϵ_{st} respectively on frequency, ν . (d, e and f) Dependence of transient creep parameter β , transient creep exponent n , and the creep strain rate, ϵ_{st} respectively on shear strain amplitudes, θ .

to 453 K can be attributed to the precipitation of intense fine ordered η -state of G.P zones up to 423 K and a disordered ϵ -state zones above this temperature to 453 K [2, 3, 15]. These fine precipitates of G.P zones act as barriers or impeding agents for moving dislocations and thus causing an increase in the creep resistance in the alloy samples [11, 14, 16–19]. The pronounced

increase in the values of n , β and ϵ_{st} at the aging temperatures range 453 to 493 K can be referred to agglomeration and partial dissolution of G.P zones. The coarse G.P zones of large size and less number make the matrix nearly depleted of zones, accordingly an easier motion of the mobile dislocations will be achieved [11, 14, 17, 18, 20]. The subsequent decrease in the values of n , β

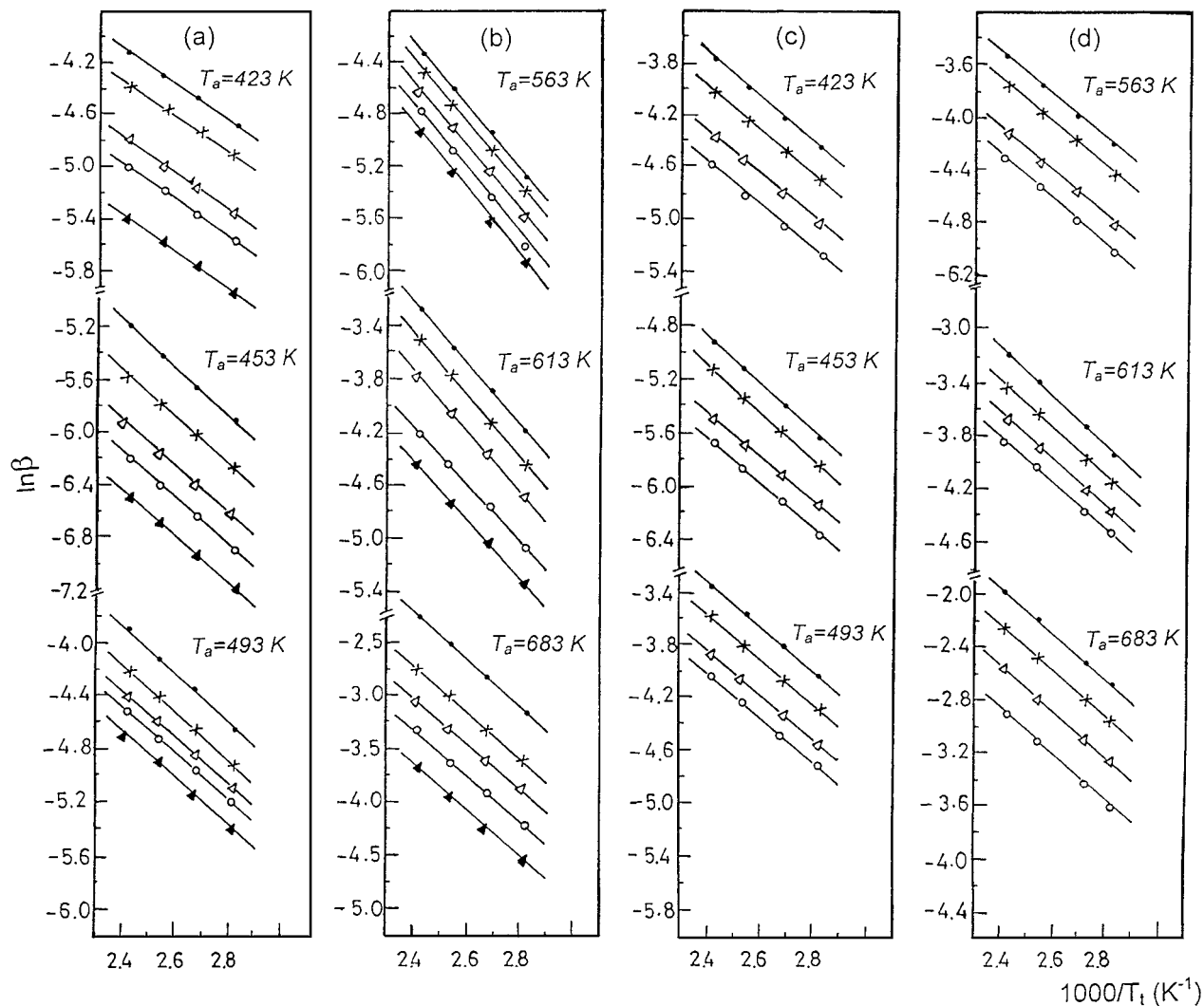


Figure 6 A plot relating $\ln \beta$ versus $10^3/T_t$ for: a and b) different frequencies and c and d) different shear strain amplitudes. The applied frequencies are: \blacktriangle) 0, \circ) 1.16, \triangle) 1.5, \times) 2 and \bullet) 2.5 Hz. The applied amplitudes are: \circ) 6.7×10^{-4} , \triangle) 7.8×10^{-4} , \times) 9.4×10^{-4} and \bullet) 11.6×10^{-4} .

and ε_{st} of specimens aged at temperatures range 493 to 563 K might be attributed to the structure variations take place in the vicinity of this temperature range. At this range of T_a , a few number of coherent γ' precipitates begin to grow not from a fully supersaturated solid solution but from regions containing the more soluble G.P zones [4]. The plate like γ' precipitates of small size concurrently with the remainder coarse zones are known [16] to block dislocations motion very effectively which eventually lead to a decrease in n , β and ε_{st} values.

At all testing temperatures worked and for both parameters of oscillations (ν and θ), the levels of n , β and ε_{st} for samples aged at 493 K are larger than those obtained for samples aged at 423 K as shown in Figs 2–4. This behavior indicates that coarse G.P zones of small number were presumably less effective to block mobile dislocation compared with ordered η -state of G.P zones of small size and large number. Also, the levels of n , β and ε_{st} for samples crept at $T_a = 453$ K are more deep as compared with their level for samples crept at $T_a = 563$ K. This behavior suggests that—under the same conditions of testing temperatures and oscillations—disordered ε -state zones inhibit the dis-

location motion by a higher rate compared with γ' precipitates of less number and small size.

The second increase in the values of n , β and ε_{st} observed in the temperatures range 563 to 613 K as clear in Figs 2–4 can be ascribed to the coarsening of γ' precipitates [6, 11, 21] whereby the number of barriers will extensively reduced and the recovery of dislocations occurs by a higher rate. The marked increase in the creep parameters at the temperatures range 613 to 683 K might be due to the transformation of metastable phases (G.P zones and γ' precipitates) to γ -phase which takes place to satisfy the equilibrium composition. Since γ -plates are very thick and widely dispersed with a minimum concentration [4, 22] so the matrix gets clean and the number of obstacles for dislocation motion should be very small [6, 21].

Increasing of β with increasing testing temperatures as shown in Fig. 3 is based on the fact that β represents the precipitation dependence of ε_{tr} on the precipitation temperature [23, 24]. So, it could be stated that increasing of testing temperatures help dislocations to overcome the precipitates that act as barriers [7]. The increase of n with the imposed oscillations, Fig. 5b and e, may be referred to the formation of new dislocation

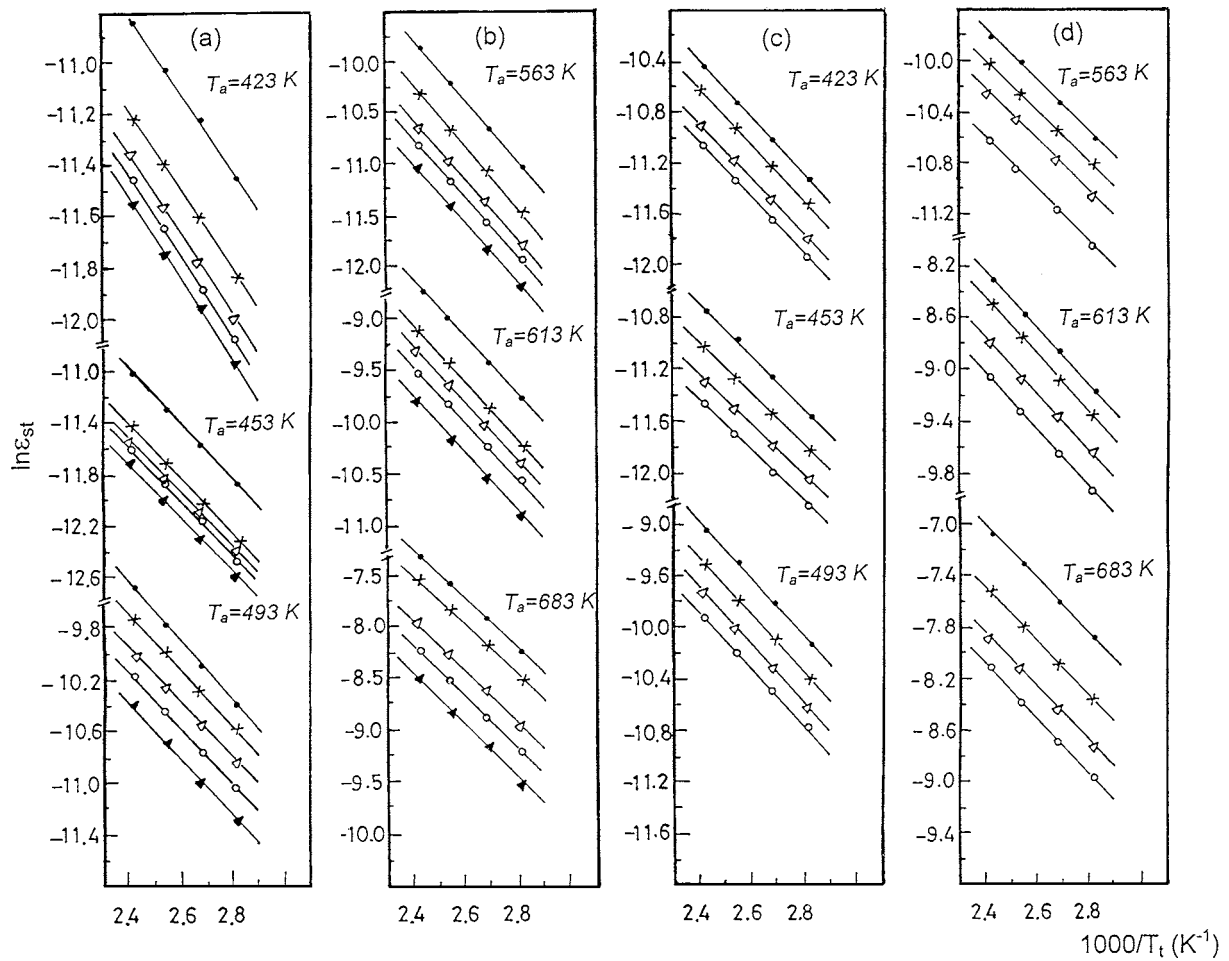


Figure 7 A plot relating $\ln \epsilon_{st}$ versus $10^3/T_w$ for: a and b) different frequencies and c and d) at different shear strain amplitude. The applied frequencies are: \blacktriangle) 0, \circ) 1.16, \triangle) 1.5, \times) 2 and \bullet) 2.5 Hz. The applied amplitudes are: \circ) 6.7×10^{-4} , \triangle) 7.8×10^{-4} , \times) 9.4×10^{-4} and \bullet) 11.6×10^{-4} .

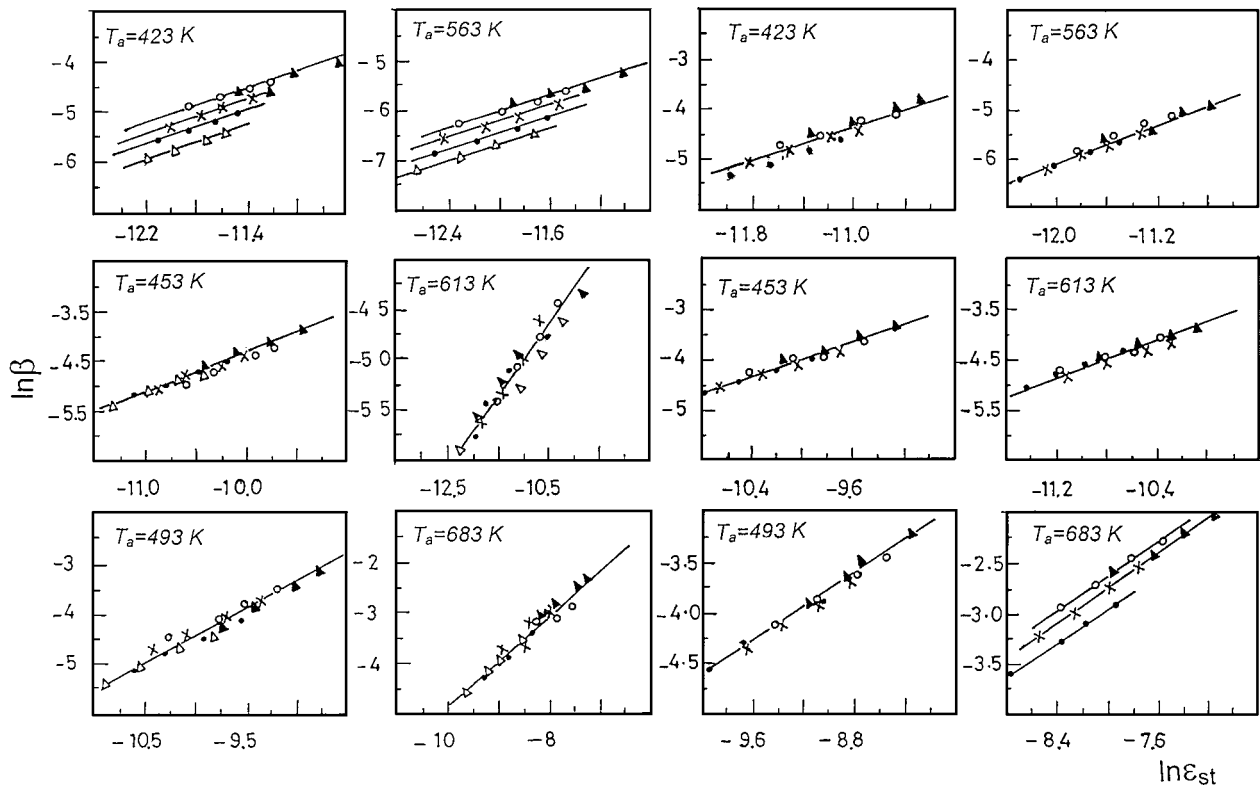


Figure 8 Relation between $\ln \beta$ and $\ln \epsilon_{st}$ at: a) different frequencies, ν and b) different shear strain amplitudes, θ . The applied frequencies are: \blacktriangle) 0, \circ) 1.16, \triangle) 1.5, \times) 2 and \bullet) 2.5 Hz. The applied amplitudes are: \circ) 6.7×10^{-4} , \triangle) 7.8×10^{-4} , \times) 9.4×10^{-4} and \bullet) 11.6×10^{-4} .

sources in the early stages of creep in the matrix [25]. The driving force for both rearrangement of these dislocation sources and annihilation of the opposite ones is accelerated by the applied stress which in addition to the effective energy applied by oscillations facilitate the movement of dislocation parallel to the applied stress direction [26].

Referring to Fig. 5a and c the observed increase in β and ε_{st} by increasing frequency of oscillations could be due to the external elastic energy provided thermally (through testing temperatures) or mechanically (with oscillations). This energy facilitates the motion of existing dislocations during the course of creep and hence, enhances the rate of recovery and shortens the duration of the creep process [7, 25]. It is well known [27] that twisting the crept samples by higher amplitudes enhances jog formation and accelerates cross slip, which is dominant in Al alloys due to the high stacking faults energy [27, 28]. So, increasing of the magnitude of shear strain amplitude is expected to hasten the tendency of jogs to clusters especially under the action of stress. Consequently, jogs of opposite signs will be annihilated resulting in a decrease in density of jogs, and an increment of the dislocation mobility a matter which increases the values of β and ε_{st} (see Fig. 5d and f).

In an attempt to determine the energy activating the transient and steady state creep processes in the present work, transient creep parameter β was assumed to vary with testing temperatures, T_t according to an Arrhenius type relation:

$$\beta = \text{constant} \exp \cdot \left(\frac{Q}{KT_t} \right) \quad (4)$$

While the values of ε_{st} satisfy the equation rate;

$$\varepsilon_{st} = \text{constant} \exp \cdot \left(\frac{Q}{KT_t} \right) \quad (5)$$

where Q is the activation energy (in kJ/mol) and K is the Boltzmann constant.

The slopes of straight lines relating $\ln \beta$ and $10^3/T_t \text{ K}^{-1}$ (Fig. 6) and $\ln \varepsilon_{st}$ versus $10^3/T_t \text{ K}^{-1}$ (Fig. 7) were calculated giving the energy activating the creep process for both transient and steady state creep stages respectively for samples crept at different frequencies (Fig. 6a and b and Fig. 7a and b) and for samples crept at different shear strain amplitudes (Fig. 6c and d and Fig. 7c and d). It is seen from Figs 6 and 7 that such plots show good parallel lines for both transient and steady state stages, predicting that the values of activation energy are frequency and shear strain amplitude independent. The calculated energies—for both creep stages—assumed values ranged from 16 to 27 kJ/mol for samples crept at different frequencies and from 14 to 23 kJ/mol for samples crept under different amplitudes. These values of activation energies are consistent with that quoted for dislocation intersection. This is acceptable since dislocation intersection process is activated by energies ranging between 15 to 25 kJ/mol for Al alloys [7, 14, 29, 30] and from 10 to 22 kJ/mol for Al-Ag alloys [11, 12, 14, 21].

Creep is a continuous process since both transient and steady state creep stages are related to each other by the relation [30, 31]:

$$\beta = \beta_0(\varepsilon_{st})^\alpha \quad (6)$$

where β_0 is a constant and α is steady state creep exponent and depends on the experimental conditions. The values of β and ε_{st} enable us to plot a relation between $\ln \beta$ and $\ln \varepsilon_{st}$ as shown in Fig. 8. A linear dependence with values of α ranged from 0.79 to 0.95 for samples crept at different frequencies and from 0.77 to 0.98 for samples crept under different amplitudes was obtained. These values of α are comparable with those obtained by Beshai *et al.* [7] (0.9–0.95) in their study on Al-1 wt% Si and Abd-El salam *et al.* [25] (0.75–0.77) in their study on Al-40 wt% Zn. The high values of α obtained may be explained as follows: In some Al alloys, the transient creep rate was found [33] to be nearly constant at the middle of primary stage. This phenomenon was considered as sub-steady state creep. T.E.M investigations confirmed that at the end of sub-steady state stage, the density of dislocations within grains increased again near grain boundaries and some of them piled-up on the slip plane. As the steady state stage starts the individual dislocations begin to take a uniform distribution and the ratio of concentration between these dislocations and vacancies do not changes giving the constant rate of steady state stage. It is therefore clear that the initial state of steady stage is almost the final state of the primary stage i.e. the mechanism controlling the transient creep strongly influences the steady state creep.

5. Conclusions

1. The observed changes in the creep parameters n , β and ε_{st} have been explained in terms of the interaction between G.P zones, γ' and γ precipitates with mobile dislocations.
2. Under the same experimental conditions coarse G.P zones of small number were presumably less effective to block mobile dislocation compared with ordered η -state of G.P zones of less size and large number.
3. Under the same conditions of testing temperatures and oscillation parameters disordered ε -state zones inhibit the dislocation motion by a higher rate compared with γ' precipitates of small number and size.
4. In both stages of creep, increasing of frequency or amplitude of imposed oscillations increase the creep parameters n , β and ε_{st} due to dislocation motion enhancement.
5. For both parameters of oscillation, the activation energies estimated indicate that the rate controlling mechanism is the dislocation interaction mechanism.
6. The high values of α suggested a high dependence of steady state creep on the transient creep stage.

References

1. J. B. COHEN, *Solid St. Phys.* **39** (1986) 131.
2. K. OSAMMURA, T. TAKAMURA, A. KABA YASHI and T. SAKURAI, *Scripta Metall.* **21** (1987) 225.
3. N. NABARRO and J. M. HOWE, *Phil. Mag.* **A 63** (1991) 645.
4. K. K. SAGOE-CRENTSIL and L. C. BROWN, *ibid.* **A 63** (1991) 477.

5. R. SHINODA, G. GRAISS and N. HABIB, *Egypt. J. Sol.* **13** (1990) 50.
6. G. GRAISS and M. A. MAHMOUD, *Cryst. Res. Technol.* **35** (2000) 95.
7. M. H. N. BESHAI, G. H. DEAF, A. M. ABDELKHALEKH, G. GRAISS and M. A. KENAWY, *Phys. Stat. Sol. (a)* **161** (1997) 65.
8. A. M. ABDELKHALEKH, Ph.D. thesis, Faculty of Girls for Arts, Science and Education, Physics Department, Ain-Shams Univ. 1997, p. 33.
9. F. ABD EL-SALAM, M. M. MOSTAFA, M. M. ELSAYED and R. H. NADA, *Phys. Stat. Sol. (a)* **144** (1994) 111.
10. G. S. AL-GANAINY, *Egypt. J. Sol.* **18** (1995) 345.
11. M. A. MAHMOUD, *Physica B* **304** (2001) 456.
12. *Idem.*, *Phys. Stat. Sol. (a)* **186**(1) (2001) 143.
13. A. MALIK, B. SCHONFELD and G. KOSTORZ, *Z. Metallk* **88** (1997) 625.
14. G. H. DEAF, S. B. YOSSEF, M. A. MAHMOUD, G. GRAISS, and M. A. KENAWY, *Phys. Stat. Sol. (a)* **158** (1996) 471.
15. G. DLUBECK, G. WENDROCK and K. PAWELZYK, *ibid.* (a) **140** (1993) 311.
16. G. H. DEAF, S. B. YOSSEF and M. A. MAHMOUD, *ibid.* (a) **168** (1998) 389.
17. G. GRAISS and M. A. MAHMOUD, *J. Mater. Sci.* **36** (2001) 1507.
18. *Idem.*, *Fizika A* **9** (2000) 137.
19. T. KANADANI and A. UMADA, *Phys. Stat. Sol. (a)* **151** (1995) K29.
20. *Idem.*, *ibid.* **148** (1995) K23.
21. G. H. DEAF, S. B. YOSSEF and M. A. MAHMOUD, *ibid.* **158** (1996) 79.
22. K. K. SAGOE-CRENTSIL and L. C. BROWN, *Metallurg. Trans.* **15A** (1984) 1969.
23. M. R. NAGY, F. ABD EL-SALAM, N. D. HABIB and R. KAMEL, *Czech. J. Phys.* **31** (1981) 937.
24. M. R. NAGY, M. S. SAKER and R. KAMEL, *Indian. J. Phys.* **A.55** (1981) 179.
25. H. JIANG, P. BOWEN and T. F. KNOTT, *J. Mater. Sci.* **34** (1999) 719.
26. F. ABD EL-SALAM, A. M. ABDELKHALEKH and R. H. NADA, *Eur. Phys. J. AP* **12** (2000) 159.
27. F. LORENZO and C. LAIRD, *Acta Metall.* **32** (1984) 681.
28. G. E. DIETER, "Mechanical Metallurgy" (McGraw Hill. Co., New York, 1986) p. 135.
29. G. H. DEAF, M. H. N. BESHAI, A. M. ABDEIKHALEKH and G. GRAISS, *Egypt. J. Sol.* **20** (1997) 61.
30. G. S. AL-GANAINY, M. T. MOSTAFA and M. R. NAGY, *Phys. Stat. Sol. (a)* **165** (1998) 185.
31. G. S. AL-GANAINY, M. R. NAGY, B. A. KHALIFA and R. AFIFI, *ibid.* **158** (1996) 463.
32. S. B. YOSSEF, A. FAWZY, M. SOBHY and G. SAAD, *Acta Phys. Slov.* **43** (1993) 431.
33. SHANCI LUI, BO WANG, CHAOQUN TANG, WANCHAN QUI ANS and FENGCHENG TIEN, *Mat. Sci. Forum.* **175** (1995) 443.

*Received 24 October 2001
and accepted 4 February 2002*